

Article

Four New Highly Oxygenated Eremophilane Sesquiterpenes from an Endophytic Fungus *Boeremia exigua* Isolated from *Fritillaria hupehensis*

Hong-Lian Ai [†], Xiao Lv [†], Ke Ye, Meng-Xi Wang, Rong Huang, Bao-Bao Shi ^{*} and Zheng-Hui Li ^{*}

School of Pharmaceutical Sciences, South-Central MinZu University, Wuhan 430074, China; aihonglian05@163.com (H.-L.A.); 2019110403@mail.scuec.edu.cn (X.L.); 2019110410@mail.scuec.edu.cn (K.Y.); 2021110499@mail.scuec.edu.cn (M.-X.W.); konglingniao1988@163.com (R.H.)

^{*} Correspondence: 2021068@mail.scuec.edu.cn (B.-B.S.); lizhenghui@mail.scuec.edu.cn (Z.-H.L.)

[†] These authors contributed equally to this work.

Abstract: Four new eremophilane-type sesquiterpenes, boeremialanes A–D (1–4) were obtained from solid substrate cultures of *Boeremia exigua* (Didymellaceae), an endophytic fungus isolated from *Fritillaria hupehensis* (Liliaceae). Boeremialanes A–C (1–3) are highly oxygenated eremophilanes with a benzoate unit attached at the C-13 position and are rarely found in nature. Their structures and absolute configurations were determined by extensive spectroscopic methods, electronic circular dichroism (ECD), and nuclear magnetic resonance (NMR) calculations with DP4+ analysis. Boeremialane D (4) potently inhibited nitric oxide production in lipopolysaccharide-treated RAW264.7 macrophages with an IC₅₀ of 8.62 μM and was more potent than the positive control, pyrrolidinedithiocarbamate (IC₅₀ = 23.1 μM).

Keywords: *Boeremia exigua*; *Fritillaria hupehensis*; eremophilanes; boeremialanes; anti-inflammatory; NO production inhibition



Citation: Ai, H.-L.; Lv, X.; Ye, K.; Wang, M.-X.; Huang, R.; Shi, B.-B.; Li, Z.-H. Four New Highly Oxygenated Eremophilane Sesquiterpenes from an Endophytic Fungus *Boeremia exigua* Isolated from *Fritillaria hupehensis*. *J. Fungi* **2022**, *8*, 492. <https://doi.org/10.3390/jof8050492>

Academic Editors: Frank Surup

Received: 18 April 2022

Accepted: 5 May 2022

Published: 8 May 2022

Publisher's Note: MDPI stays neutral with regard to jurisdictional claims in published maps and institutional affiliations.



Copyright: © 2022 by the authors. Licensee MDPI, Basel, Switzerland. This article is an open access article distributed under the terms and conditions of the Creative Commons Attribution (CC BY) license (<https://creativecommons.org/licenses/by/4.0/>).

1. Introduction

Eremophilane-type derivatives are structurally irregular and bicyclic natural products belonging to a small sesquiterpene family [1,2]. These eremophilane sesquiterpenes are biogenetically derived from farnesyl diphosphate in association with a methyl migration [3] and consist of three isoprene subunits [4]. The structural diversity of eremophilane analogs is due to oxidation occurring at different sites along the isopropyl side chain and bicyclic backbone to generate alcohol [5], acid [6], ester [7–9], furan [10,11], and lactone functionalities, with some of the alcohols further glycosylated [12]. Since the first eremophilane-type sesquiterpene was isolated from the wood oil of *Eremophila mitchellii* in 1932 [13], more than 650 biologically active eremophilane derivatives have been obtained [2,14]. In addition to the related analogs obtained from terrestrial plants [15,16] and marine fungi [17,18], plant endophytic fungi are recognized as a new source of derivatives eremophilane [19,20]. Due to their special structural features and various functional groups, eremophilane-type sesquiterpenes possess a lot of biological activities such as anti-inflammatory [21], anti-tumor [10], and antibacterial [22,23] activities, which have received increasing interest in the recent years. As part of our ongoing efforts to discover bioactive terpenoids derived from endophytic fungi [24–27], a chemical investigation on the cultural broth of *B. exigua* in rice medium was carried out. As a result, four new highly oxygenated eremophilane-type sesquiterpenes, boeremialanes A–D (1–4), were isolated from cultures of the fungus *B. exigua*. The new structures were established by extensive spectroscopic methods, ECD and NMR calculations, as well as DP4+ analysis. All compounds were tested for their anti-inflammatory activities on nitric oxide production in LPS-induced RAW264.7 macrophages. Herein, details of the isolation, structural elucidation and bioactivities of the compounds are reported.

2. Materials and Methods

2.1. General Experimental Procedures

Optical rotations were measured with an Autopol IV polarimeter (Rudolph, Hackettstown, NJ, USA). UV spectra were measured on a UV-2450 spectrometer (Hitachi High-Technologies, Tokyo, Japan). CD spectra were recorded with an Applied Photophysics spectrometer (Chirascan, New Haven, CT, USA). One-dimensional and 2D spectra were recorded on a Bruker AV-600 spectrometer (Bruker, Karlsruhe, Germany) with TMS as an internal standard. HRESIMS spectra were recorded on Q Exactive Orbitrap mass spectrometer (ThermoFisher Scientific, Waltham, MA, USA). Medium pressure liquid chromatography (MPLC) was performed on a Biotage SP1 System and column packed with RP-18 gel (Biotage, Uppsala, Sweden). Silica gel (Qingdao Marine Chemical Factory, Qingdao, China), RP-18 gel (Fuji Silysia Chemical Factory, Kasugai, Japan), and Sephadex LH-20 (Pharmacia Fine Chemical Factory, Uppsala, Sweden) were used for column chromatography (CC). Semi-preparative HPLC experiments were carried on Agilent 1260 HPLC with Zorbax SB-C₁₈ column (Agilent, Palo Alto, CA, USA, 5 μ m, 9.4 mm \times 150 mm). Fractions were monitored by TLC (GF 254, Qingdao Haiyang Chemical Factory, Qingdao, China), and spots were visualized by heating silica gel plates sprayed with vanillin and 10% H₂SO₄ in EtOH.

2.2. Culture and Fermentation of Fungal Material

The strain *B. exigua* was isolated from the healthy leaf tissue of *Fritillaria hupehensis* Hsiao. It was identified by Dr. Hong-Lian Ai (South-Central MinZu University). The ITS sequence of this strain is almost identical to the strain deposited in Genbank with accession number MT154621.1 (max identity: 100%, query cover: 100%). The fungal specimen is deposited at South-Central MinZu University, China. The strain was cultured on PDA medium for 8 days, and then was cut into small pieces to incubate solid rice medium to culture for further 30 days at 25 °C (50 g rice, 50 mL water, in each 500 mL Erlenmeyer flask, the total weight of rice was 17 kg).

2.3. Extraction and Isolation

The rice fermentation product of *B. exigua* (17 kg) was extracted five times with methanol to yield a crude extract after evaporation under vacuum. The crude extract was partitioned between water and EtOAc to give an EtOAc layer. The extract (800 g) of the organic layer was subjected to column chromatography over silica gel (200–300 mesh, CH₂Cl₂-MeOH, step gradient elution 1:0, 20:1, 10:1, 5:1, 2:1, 1:1, and 0:1) to obtain six fractions (A–F). Fr. C (35.8 g) was fractionated by MPLC over an RP-18 silica gel column and eluted with MeOH-H₂O (from 20:80 to 90:10, *v/v*) to yield five subfractions (C₁–C₅). Fraction C₁ (5.8 g) was separated on a silica gel column (200–300 mesh, CH₂Cl₂-MeOH, step gradient elution 10:1, 4:1, 2:1, and 1:1) to give four subfractions (Fr. C₁₋₁–Fr. C₁₋₄). Then, Fr. C₁₋₁ was purified by semi-preparative HPLC (CH₃CN/H₂O from 25:75 to 35:65 over 30 min) to obtain compound **4** (2.0 mg, retention time (*t*_R) = 12.0 min). Fr. C₁₋₂ was purified by semi-preparative HPLC (CH₃CN/H₂O from 28:72 to 36:64 over 28 min) to obtain compound **1** (5.1 mg, *t*_R = 15.6 min), compound **2** (7.2 mg, *t*_R = 17.8 min), and compound **3** (8.1 mg, *t*_R = 19.7 min).

Boeremialane A (1): Yellowish oil; $[\alpha]_D^{27}$ 102.5 (*c* 0.1, MeOH); UV (MeOH) λ_{\max} (log ϵ) 205 (3.61), 230 (3.46) nm; ¹H NMR (600 MHz) and ¹³C NMR (150 MHz, methanol-*d*₄), see Table 1; HRESIMS (positive) *m/z* 483.16220 [M + Na]⁺ (calcd for C₂₄H₂₈O₉Na⁺, 483.16255).

Boeremialane B (2): Yellowish oil; $[\alpha]_D^{27}$ 50.0 (*c* 0.1, MeOH); UV (MeOH) λ_{\max} (log ϵ) 210 (3.44), 235 (3.16) nm; ¹H NMR (600 MHz) and ¹³C NMR (150 MHz, methanol-*d*₄), see Table 1; HRESIMS (positive) *m/z* 441.15195 [M + Na]⁺ (calcd for C₂₂H₂₆O₈Na⁺, 441.15199).

Boeremialane C (3): Yellowish oil; $[\alpha]_D^{27}$ 216.0 (*c* 0.1, MeOH); UV (MeOH) λ_{\max} (log ϵ) 205 (3.75), 250 (3.80) nm; ¹H NMR (600 MHz) and ¹³C NMR (150 MHz, methanol-*d*₄), see Table 1; HRESIMS (positive) *m/z* 441.15182 [M + Na]⁺ (calcd for C₂₂H₂₆O₈Na⁺, 441.15199).

Boeremialane D (**4**): Yellow amorphous powder; $[\alpha]_D^{27}$ 136.0 (c 0.1, MeOH); UV (MeOH) λ_{\max} (log ϵ) 240 (3.47) nm; ^1H NMR (600 MHz) and ^{13}C NMR (150 MHz, methanol- d_4), see Table 1; HRESIMS (positive) m/z 345.13064 $[\text{M} + \text{Na}]^+$ (calcd for $\text{C}_{17}\text{H}_{22}\text{O}_6\text{Na}^+$, 345.13086).

Table 1. ^1H and ^{13}C NMR Spectroscopic Data for **1** and **2** in Methanol- d_4 (δ in ppm, J in Hz).

No.	δ_{H} (1) ^a	δ_{C} (1) ^b	δ_{H} (2) ^a	δ_{C} (2) ^b
1	2.41 (tdd, 14.4, 5.0, 1.9) 2.24 (dt, 14.4, 4.1)	31.6, CH ₂	2.51 (tdd, 14.4, 5.0, 1.9) 2.28 (dt, 14.4, 3.5)	31.6, CH ₂
2	2.03 (dd, 12.3, 4.4) 1.27 (ddd, 12.3, 5.0, 4.1)	36.2, CH ₂	2.07 (dd, 12.2, 4.4) 1.29 (ddd, 12.2, 5.0, 3.5)	36.3, CH ₂
3	3.44 (td, 10.5, 4.4)	71.1, CH	3.53 (td, 10.5, 4.4)	71.1, CH
4	1.63 (dq, 10.5, 6.7)	45.9, CH	1.70 (dq, 10.5, 6.7)	46.0, CH
5		42.2, C		42.3, C
6	3.80 (s)	63.9, CH	3.91 (s)	64.1, CH
7		62.9, C		62.8, C
8		195.5, C		195.4, C
9	5.61 (d, 1.9)	121.8, CH	5.66 (d, 1.9)	121.8, CH
10		166.5, C		166.5, C
11		73.9, C		74.2, C
12	4.19 (d, 11.6) 3.76 (d, 11.6)	65.6, CH ₂	4.17 (d, 11.6) 3.81 (d, 11.6)	65.5, CH ₂
13	4.64 (d, 11.5) 4.59 (d, 11.5)	69.3, CH ₂	4.83 (d, 11.7) 4.44 (d, 11.7)	67.5, CH ₂
14	0.64 (s)	18.3, CH ₃	1.03 (s)	19.0, CH ₃
15	1.16 (d, 6.7)	11.6, CH ₃	1.23 (d, 6.7)	11.6, CH ₃
1'		169.6, C		168.1, C
2'		134.3, C		132.4, C
3'		132.8, C	7.37 (dd, 2.6, 1.3)	117.3, CH
4'	7.77 (dd, 6.4, 2.1)	130.3, CH		158.8, C
5'	7.62 (td, 6.4, 2.7)	129.7, CH	7.00 (dd, 7.9, 2.6)	121.3, CH
6'	7.61 (td, 6.4, 2.1)	132.9, CH	7.25 (t, 7.9)	130.5, CH
7'	7.59 (dd, 6.4, 2.7)	132.3, CH	7.44 (dd, 7.9, 1.3)	121.8, CH
COOCH ₃	3.85 (s)	53.5, CH ₃		
COOCH ₃		168.9, C		

^a Recorded at 600 MHz, ^b Recorded at 150 MHz.

2.4. Quantum Chemical Calculations

The initial conformational analysis of compounds **1–4** was performed using the Monte Carlo search algorithm via the MMFF94 molecular mechanics force field [28], with the aid of the Spartan 16 program package that resulted in some relatively favorable conformations with an energy range of 3 kcal/mol above the global minimum. The minimum energy conformers of the resulting force field were optimized in vacuum with the M06-2X/def2-SVP level, and implemented in the Gaussian 09 software package by the Density functional theory [29]. At the same time, harmonic vibrational frequencies were also measured to confirm the lack of imaginary frequencies of the finally optimized conformers. These primary conformations were subjected to theoretical calculations of ECD utilizing time-dependent density functional theory (TDDFT) calculations at the M06-2X/def2-SVP level in MeOH using the polarizable continuum model (PCM) solvent model. The energies, oscillator strengths, and rotational strengths of each conformation were determined with the Gaussian 09 software package. Theoretical calculations of ECD spectra for each part were then approximated by the Gaussian distribution. The final ECD spectrum of the individual conformers was summed up on the basis of the Boltzmann-weighted population contribution by the SpecDisv1.71 [30]. DFT GIAO ^{13}C NMR calculations were performed on the mPW1PW91/6-31 + G(d,p)/M06-2X/def2-SVP level of theory [31]. The solvent effect was accounted for by using methanol in the calculations to mimic the experimental conditions. The ^{13}C NMR chemical shifts in compound **1** were considered the average values of the same atoms in the different conformers. We took the relative Gibbs free energy

as the weighting factor and used the Boltzmann distribution to find the average values. The overall theoretical NMR data were analyzed using DP4+ probability [32].

2.5. Nitric Oxide Production Inhibitory Assay

The anti-inflammatory effect of Raw264.7 macrophages was studied and cultured in Dulbecco's modified eagle medium (DMEM, HyClone, Logan, UT, USA) with 10% fetal bovine serum (FBS, PAN, Aidenbach, Germany) in a humidified incubator (5% CO₂, 37 °C). RAW264.7 cells (5 × 10⁴ cells/well) were seeded into a 96-well multiplate for 12 h. After 12 h of incubation, the cells were treated with LPS (1 µg/mL) and different concentrations of the tested compounds (1–4, 20 µM) for 18 h. A Griess reagent kit (Promega, Madison, WI, USA) was used to measure the amount of nitrite, a stable metabolite of Nitric Oxide (NO), in the supernatants. Briefly, 50 µL of each culture medium was added to a 96-well plate, and then the same volume of sulfanilamide solution was added. After incubation at room temperature for 5 min, 50 µL of N-1-naphthylethylenediamine dihydrochloride solution was added to all wells. The absorption at 540 nm was measured by a microplate reader after 10 min incubation at room temperature [33]. The IC₅₀ values were calculated by GraphPad Prism 6 software. Cell viability was determined with the MTT (3-[4,5-dimethylthiazol-2-yl]-2,5 diphenyl tetrazolium bromide) assay. Pyrrolidine dithiocarbamate (PDTC, Sigma–Aldrich, St Louis, MO, USA) was used as a positive control.

3. Results and Discussion

Boeremialane A (**1**) was obtained as a yellowish oil, and the molecular formula of compound **1** was determined to be C₂₄H₂₈O₉ from the HRESI mass spectrum ([M + Na]⁺ data, found 483.16220, calcd. 483.16255). The ¹H and ¹³C NMR data of compound **1** indicated the presence of two methyl groups (δ_C 11.6 and 18.3), four methylene groups (δ_C 31.6, 36.2, 65.6, and 69.3), eight methine groups (δ_C 71.1, 45.9, 63.9, 121.8, 130.3, 129.7, 132.9, and 132.3), one carbonyl (δ_C 195.5), two ester carbonyls (δ_C 169.6 and 168.9), three sp³ quaternary carbons (δ_C 42.2, 62.9, and 73.9), and three sp² quaternary carbons (δ_C 166.5, 134.3, and 132.8) (Table 1, Figures S5–S10). In the HMBC spectrum (Figures 1 and 2), a singlet for the Me-14 at δ_H 0.64 (3H, s, H-14) showed correlations to C-4 (δ_C 45.9), C-6 (δ_C 63.9), C-10 (δ_C 166.5), and a sp³ quaternary carbon at δ_C 42.2 (C-5). This was very important for the establishment of the three C-C bonds of C-4, C-10, and C-6 with C-5. In addition, the HMBC spectrum showed correlations from H-1 (δ_H 2.41 and 2.24) to C-5 and C-10, and the ¹H-¹H COSY spectrum analysis (H-1/H-2/H-3/H-4/H-15) together with a characteristic oxygenated methine carbon (δ_C 71.1, C-3) determined a 1,2,3,3,4-pentasubstituted cyclohexane ring of compound **1**. A 2-cyclohexen-1-one ring was inferred by the HMBC correlations from H-6 (δ_H 3.80) to C-5, C-7, C-8, and C-10 and from H-9 (δ_H 5.61) to C-5 and C-7, with the connection to the cyclohexane ring by the C-5/C-10 position on the basis of the HMBC correlations of H-1/C-9 and H-4/C-6 (Figure 2). The HMBC correlations from H-12 (δ_H 4.19 and 3.76) to C-11 and C-13 and from H-13 (δ_H 4.64 and 4.59) to C-11 and C-12 together with the downfield shifts of C-11 (δ_C 73.9), C-12 (δ_C 65.6), and C-13 (δ_C 69.3) indicated the existence of a highly oxidized propane group, which was linked to the position of C-7, as evidenced by the HMBC correlations from H-12 to C-7 and from H-13 to C-7. These data, as well as other HMBC correlations, suggested that unit A was a tetrol phaseolinone [34], which had been previously isolated from *Macrophomina phaseolina*.

For unit B, the ¹H NMR spectrum of compound **1** revealed the signals for four aromatic protons (δ_H 7.77, 7.62, 7.61, and 7.59). In the ¹H-¹H COSY spectrum, a disubstituted benzene ring was identified by four continuous aromatic protons at δ_H 7.77 (1H, d, H-4'), 7.62 (1H, t, H-5'), 7.61 (1H, t, H-6'), and 7.59 (1H, d, H-7'), and two aromatic doublets and two aromatic triplets with the same coupling constant (*J* = 6.4 Hz) indicated an ortho-disubstituted benzene group. A carbomethoxy substituent in the benzene ring was identified by the HMBC correlations from H-4' to the carbomethoxy substituent (δ_C 168.9). Similarly, an ester carbonyl carbon (δ_C 169.6) was positioned at C-2' based on observed cross-peaks at H-7'/C-1'. The HMBC correlations from H-13 to the ester carbonyl carbon

(C-1') confirmed the 13,1'-ester linkage of the two substructures. Thus, the planar structure of compound **1** was elucidated as shown in Figure 1.

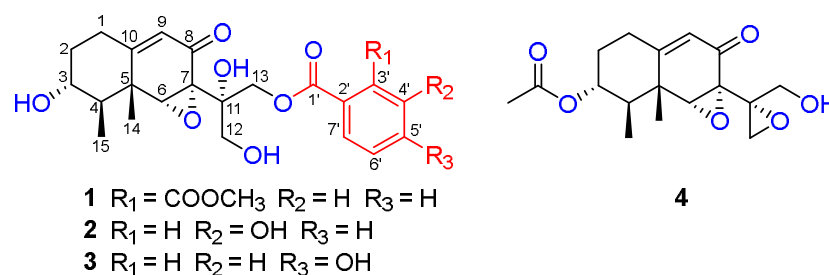


Figure 1. Chemical structures of compounds 1–4.

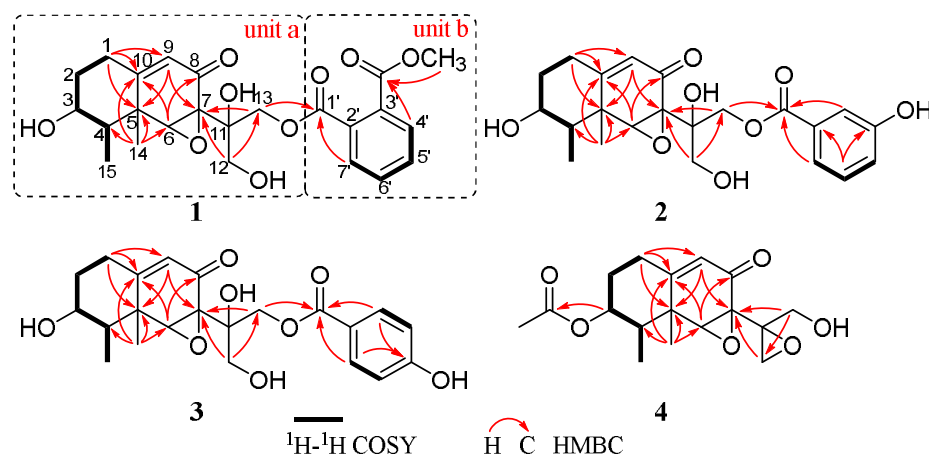


Figure 2. Key HMBC and ¹H-¹H COSY correlations of compounds 1–4.

The configuration of boeremialane A (**1**) was established by ROESY experiments and quantum chemistry calculations. The ROESY correlations of H-3/H₃-15, H-3/H₃-14, H-6/H₃-14, and H-6/H₃-15 suggested that they were β-oriented (Figure 3). In addition, to determine the configuration of C-11 in the flexible bond, nuclear magnetic resonance (NMR) calculations of two epimers, 11S-**1** and 11R-**1**, were carried out. The two epimers were subjected to a strict conformational screening procedure; then, the NMR chemical shifts were calculated at the mPW1PW91/6-31 + G(d,p)//M06-2X/def2-SVP level of theory with the PCM solvent in methanol. The DP4+ analysis identified 11S-**1** as the most likely structure of compound **1** with 100.00% DP4+ probability (all data) (Figure 4 and Table S1). Finally, the absolute configuration of compound **1** was resolved by comparing the calculated and experimental ECD data using time-dependent density-functional theory (TDDFT). The theoretical spectrum of compound **1** showed an excellent fit with the experimental plot recorded in MeOH (Figures 5 and S1), which supported an absolute configuration of 3R, 4R, 5R, 6R, 7S, and 11S. Thus, the structure of compound **1** was determined, and it was named boeremialane A.

Boeremialane B (**2**) was obtained as a yellowish oil, and the molecular formula was determined to be C₂₂H₂₆O₈ from the HRESI mass spectrum data ([M + Na]⁺, found 441.15195, calcd. 441.15199). The ¹H and ¹³C NMR data of compound **2** indicated the presence of two methyl groups (δ_C 11.6 and 19.0), four methylene groups (δ_C 31.6, 36.3, 65.6, and 67.5), eight methine groups (δ_C 71.1, 46.0, 64.1, 121.8, 117.3, 121.3, 130.5, and 121.8), one carbonyl (δ_C 195.4), one ester carbonyl (δ_C 168.1), three sp³ quaternary carbons (δ_C 42.3, 62.8, and 74.2), and three sp² quaternary carbons (δ_C 166.5, 132.4, and 158.8) (Table 1 and Figures S12–S17). The ¹H and ¹³C NMR data of compound **2** were structurally similar to those of compound **1**, except for the absence of a carbomethoxy group at δ_C 168.9 and 53.5 in compound **1** and the presence of an additional hydroxy group in compound **2**. The hydroxyl group at C-4' was evident from the downfield shift of C-4' (δ_C 158.8) as well as the HMBC

correlations from H-13 to the sp^2 quaternary carbon (C-4') (Figure 2). The relative configuration of compound **2** was the same as that found in compound **1** based on the ROESY correlations of H-3/H₃-15, H-3/H₃-14, H-6/H₃-14, and H-6/H₃-15 (Figure 3). Finally, the absolute configuration of **2** was determined by ECD calculations on the M06-2X/def2-SVP (IEFPCM, MeOH) level of theory. The experimental ECD spectrum of compound **2** fits well with the calculated spectrum of 3*R*, 4*R*, 5*R*, 6*R*, 7*S*, and 11*S*-**2** (Figures 5 and S2). Therefore, the structure of compound **2** was determined, and it was given the name boeremialane B.

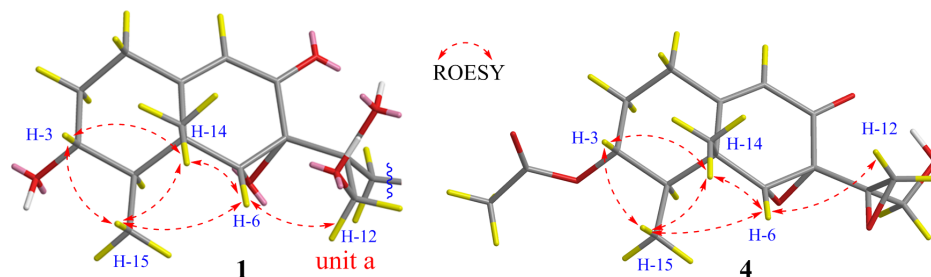


Figure 3. Key ROESY correlations of compounds **1** and **4**.

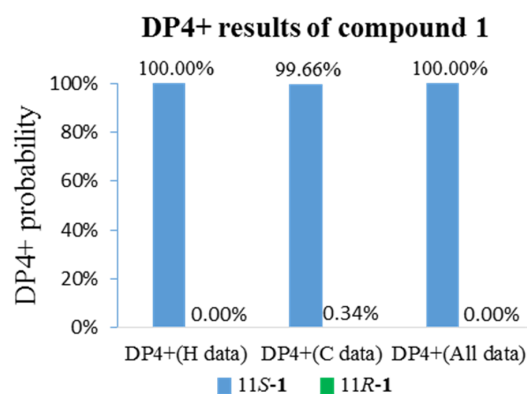


Figure 4. qccNMR coupled with DP4+ probability analysis of compound **1**.

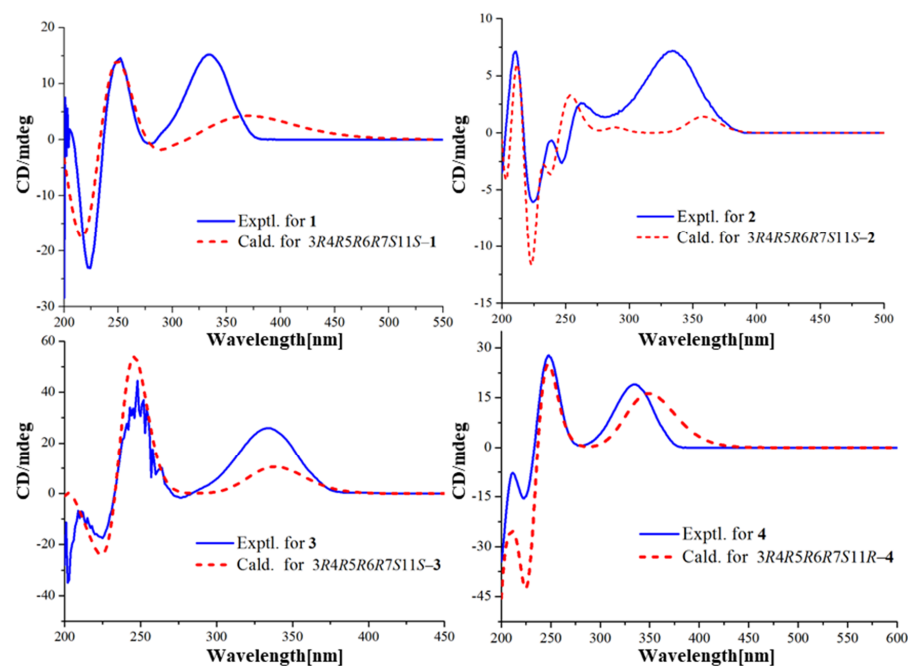


Figure 5. Experimental and calculated ECD spectra of compounds **1**–**4** at the M06-2X/def2-SVP level in methanol.

Boeremialane C (**3**) has a molecular formula of $C_{35}H_{40}O_8$ according to its HRESIMS ion at m/z 441.15182 $[M + Na]^+$ (calcd for $C_{22}H_{26}O_8Na$, 441.15199). The 1H and ^{13}C NMR data of **3** (Table 2 and Figures S19–S24) were structurally similar to those of compound **2**, except for the presence of a para-substituted benzene ring of the benzoate unit. This difference was supported by the HMBC correlations from H-3' (7') (δ_H 7.81) to C-1' (δ_C 168.4) and C-5' (δ_C 165.9) along with the COSY correlations between H-3' (7')/H-4' (6') (δ_H 6.74) (Figure 2). The ECD spectrum of compound **3** was similar to that of compound **1** with negative exciton coupling at 211 nm and positive exciton coupling at 241 nm (Figure S33), which indicated that they share the identical absolute configuration. Therefore, the absolute configuration of **3** was defined as 3*R*, 4*R*, 5*R*, 6*R*, 7*S*, and 11*S*. This presumption was confirmed by comparative analysis of calculated and experimental ECD spectra. The experimental ECD spectrum of **3** fits well with the calculated spectrum of 3*R*, 4*R*, 5*R*, 6*R*, 7*S*, and 11*S*-**3** (Figures 5 and S3). Thus, the structure of **3** was determined and named boeremialane C.

Table 2. 1H and ^{13}C NMR Spectroscopic Data for **3** and **4** in Methanol- d_4 (δ in ppm, J in Hz).

No.	δ_H (3) ^a	δ_C (3) ^b	δ_H (4) ^a	δ_C (4) ^b
1	2.50 (tdd, 14.4, 4.8, 1.8) 2.28 (dt, 14.4, 3.5)	31.6, CH ₂	2.41 (tdd, 14.6, 5.0, 1.8) 2.39 (dt, 14.6, 4.0)	31.2, CH ₂
2	2.07 (dd, 12.5, 4.4) 1.29 ddd, 12.5, 4.8, 3.5	36.3, CH ₂	2.15 (dd, 12.3, 4.4) 1.40 (ddd, 12.3, 5.0, 4.0)	32.5, CH ₂
3	3.53 (td, 10.6, 4.4)	71.1, CH	4.91 (td, 10.5, 4.4)	74.2, CH
4	1.69 (dq, 10.6, 6.8)	45.9, CH	1.95 (dq, 10.5, 6.8)	43.1, CH
5		42.2, C		42.4, C
6	3.89 (s)	64.1, CH	3.63 (s)	65.5, CH
7		62.8, C		62.1, C
8		195.3, C		194.2, C
9	5.65 (d, 1.8)	121.8, CH	5.75 (d, 1.8)	121.7, CH
10		166.4, C		165.4, C
11		74.3, C		59.0, C
12	4.17 (d, 11.6) 3.81 (d, 11.6)	65.5, CH ₂	2.87 (d, 5.1) 2.66 (d, 5.1)	48.3, CH ₂
13	4.82 (d, 11.7) 4.39 (d, 11.7)	67.2, CH ₂	4.07 (d, 12.3) 3.72 (d, 12.3)	62.0, CH ₂
14	1.02 (s)	19.1, CH ₃	1.26 (s)	18.6, CH ₃
15	1.22 (d, 6.8)	11.6, CH ₃	1.14 (d, 6.8)	11.4, CH ₃
1'		168.4, C		
2'		120.5, C		
3'	7.81 (d, 8.8)	133.1, CH		
4'	6.74 (d, 8.8)	116.8, CH		
5'		165.9, C		
6'	6.74 (d, 8.8)	116.8, CH		
7'	7.81 (d, 8.8)	133.1, CH		
CH ₃ CO			2.06 (s)	21.0, CH ₃
CH ₃ CO				172.4, C

^a Recorded at 600 MHz, ^b Recorded at 150 MHz.

Boeremialane D (**4**) was obtained as a yellow amorphous powder, and the molecular formula, $C_{17}H_{22}O_6$, was determined by (+)-HRESIMS, which showed an $[M + Na]^+$ ion at m/z 345.13064 (calcd for $C_{17}H_{22}O_6Na$: 345.13086). The 1H and ^{13}C NMR data of compound **4** indicated the presence of three methyl groups (δ_C 18.6, 11.4, and 21.0), four methylene groups (δ_C 31.2, 32.5, 48.3, and 62.0), four methine groups (δ_C 74.2, 43.1, 65.5, and 121.7), one carbonyl (δ_C 194.2), one ester carbonyl (δ_C 172.4), three sp³ quaternary carbons (δ_C 42.4, 62.1, and 59.0), and one sp² quaternary carbon (δ_C 165.4) (Table 2 and Figures S26–S31). The 1H and ^{13}C NMR data of compound **4** were structurally similar to those of phaseolinone [35], except for the appearance of an additional acetyl group in compound **4**. The attachment of this acetyl group at C-3 was supported by the HMBC correlation from the H-3 to the ester carbonyl carbons (δ_C 172.4). The relative configuration of compound **4** was the same as that found in compound **1** based on the ROESY

correlations of H-3/H₃-15, H-3/H₃-14, H-6/H₃-14, and H-6/H₃-15 (Figure 3). Similar to compound 3, the tendencies of the ECD curves of compounds 4 and 1 with negative exciton coupling at 225 nm and positive exciton coupling at 250 and 337 nm were relatively consistent (Figure S33, Supporting Information), which indicated that they have an the identical absolute configuration. In addition, the identity of the measured ECD and calculated ECD spectrum of compound 4 further confirmed this conclusion (Figures 5 and S4). Therefore, the structure of compound 4 was determined, and it was given the name boeremialane D.

All compounds were evaluated for their inhibition of NO production in LPS-treated RAW264.7 macrophages. As a result, compound 4 showed certain inhibitory activity with IC₅₀ values of 8.62 μM, which was more potent than the positive control, pyrrolidinedithiocarbamate (IC₅₀ = 23.1 μM) (Figure 6).

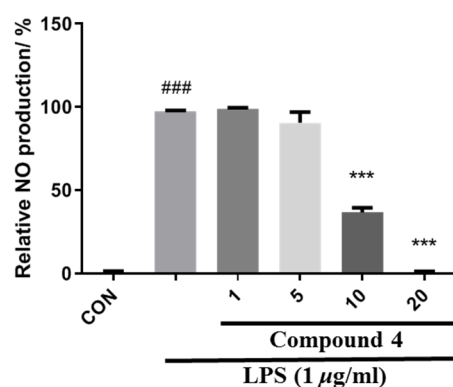


Figure 6. Effects of compound 4 isolated from *B. exigua* on NO production in LPS-stimulated RAW 264.7 macrophages. Cells were pretreated with the indicated concentrations of the isolates for 1 h and then stimulated with LPS (1 μg/mL) for 24 h. The NO levels in the culture medium were measured by the MTT assay. ### $p < 0.0001$ vs. control. *** $p < 0.0001$ vs. LPS-stimulated group.

4. Conclusions

In summary, the structures of four new eremophilane-type sesquiterpenes (1–4) were unambiguously determined by analyses of their HRESI and NMR spectroscopic data, with the absolute configuration being determined by quantum chemistry calculations. Boeremialanes A–C (1–3) are highly oxygenated eremophilanes with the benzoate unit attached at the C-13 position, and only one such natural compound has been discovered to date [35]. Compound 4 exhibited potent inhibition against NO production in LPS-activated RAW 264.7 macrophages, suggesting that it is a new chemical entity for anti-inflammatory effects. The present research provides new insights into understanding the structural diversity and interesting biological activities of eremophilane sesquiterpenes.

Supplementary Materials: The following are available online at <https://www.mdpi.com/article/10.3390/jof8050492/s1>. Table S1. DP4+ analysis results of 1a (Isomer 1) and 1b (Isomer 2). Table S2. Experimental and calculated ¹³C NMR chemical shifts of 1a and 1b. Table S3. Important thermodynamic parameters of the M06-2X/def2-SVP optimized conformers of 1a in the gas phase. Table S4. Conformational analysis of the M06-2X/def2-SVP optimized conformers of 1a in the gas phase (T = 298.15 K). Table S5. Important thermodynamic parameters of the M06-2X/def2-SVP optimized conformers of 2 in the gas phase. Table S6. Conformational analysis of the M06-2X/def2-SVP optimized conformers of 2 in the gas phase (T = 298.15 K). Table S7. Important thermodynamic parameters of the M06-2X/def2-SVP optimized conformers of 3 in the gas phase. Table S8. Conformational analysis of the M06-2X/def2-SVP optimized conformers of 3 in the gas phase (T = 298.15 K). Table S9. Important thermodynamic parameters of the M06-2X/def2-SVP optimized conformers of 4 in the gas phase. Table S10. Conformational analysis of the M06-2X/def2-SVP optimized conformers of 4 in the gas phase (T = 298.15 K). Table S11. Cartesian coordinates for the low-energy optimized conformers of 1–4 at M06-2X/def2-SVP level. Figure S1. Experimental ECD spectra and calculated ECD spectra of 1. Figure S2. Experimental ECD spectra and calculated ECD spectra of 2. Figure S3. Experimental ECD spectra and calculated ECD spectra of 3. Figure S4. Experimental ECD spectra and calculated

ECD spectra of **4**. Figure S5. ^1H NMR spectrum of **1** in CD_3OD . Figure S6. ^{13}C NMR spectrum of **1** in CD_3OD . Figure S7. HSQC spectrum of **1** in CD_3OD . Figure S8. HMBC spectrum of **1** in CD_3OD . Figure S9. COSY spectrum of **1** in CD_3OD . Figure S10. ROESY spectrum of **1** in CD_3OD . Figure S11. HRMS spectrum of **1**. Figure S12. ^1H NMR spectrum of **2** in CD_3OD . Figure S13. ^{13}C NMR spectrum of **2** in CD_3OD . Figure S14. HSQC spectrum of **2** in CD_3OD . Figure S15. HMBC spectrum of **2** in CD_3OD . Figure S16. COSY spectrum of **2** in CD_3OD . Figure S17. Roesy spectrum of **2** in CD_3OD . Figure S18. HRMS spectrum of **2**. Figure S19. ^1H NMR spectrum of **3** in CD_3OD . Figure S20. ^{13}C NMR spectrum of **3** in CD_3OD . Figure S21. HSQC spectrum of **3** in CD_3OD . Figure S22. HMBC spectrum of **3** in CD_3OD . Figure S23. COSY spectrum of **3** in CD_3OD . Figure S24. Roesy spectrum of **3** in CD_3OD . Figure S25. HRMS spectrum of **3**. Figure S26. ^1H NMR spectrum of **4** in CD_3OD . Figure S27. ^{13}C NMR spectrum of **4** in CD_3OD . Figure S28. HSQC spectrum of **4** in CD_3OD . Figure S29. HMBC spectrum of **4** in CD_3OD . Figure S30. COSY spectrum of **4** in CD_3OD . Figure S31. Roesy spectrum of **4** in CD_3OD . Figure S32. HRMS spectrum of **4**. Figure S33. CD spectrum of **1–4** in MeOH .

Author Contributions: H.-L.A. contributed to isolation and cultivation of fungi. X.L. contributed to the extraction, isolation, and identification of the samples. K.Y. contributed to the isolation of the samples. M.-X.W. and R.H. contributed to the bioactivity tests. B.-B.S. contributed to the quantum chemical calculation and the preparation of the manuscript. H.-L.A. and Z.-H.L. designed the experiments. All authors have read and agreed to the published version of the manuscript.

Funding: This work was financially supported by the National Natural Science Foundation of China (31870513) and the Fundamental Research Funds for the Central Universities, South-Central MinZu University (CZD21003).

Institutional Review Board Statement: Not applicable.

Informed Consent Statement: Not applicable.

Data Availability Statement: Not applicable.

Acknowledgments: The authors thank the Analytical & Measuring Centre, South-Central MinZu University for the spectral measurements.

Conflicts of Interest: The authors declare no conflict of interest. The funders had no role in the design of the study; in the collection, analyses, or interpretation of data; in the writing of the manuscript, or in the decision to publish the results.

References

1. Fraga, B.M. Natural sesquiterpenoids. *Nat. Prod. Rep.* **2009**, *26*, 1125–1155. [[CrossRef](#)] [[PubMed](#)]
2. Wu, L.; Liao, Z.X.; Liu, C.; Jia, H.Y.; Sun, J.Y. Eremophilane Sesquiterpenes from the Genus *Ligularia*. *Chem. Biodivers.* **2016**, *13*, 645–671. [[CrossRef](#)] [[PubMed](#)]
3. Schenk, D.J.; Starks, C.M.; Manna, K.R.; Chappell, J.; Noel, J.P.; Coates, R.M. Stereochemistry and deuterium isotope effects associated with the cyclization-rearrangements catalyzed by tobacco *epiaristolochene* and *hyoscyamus premnaspirodiene* synthases, and the chimeric CH_4 hybrid cyclase. *Arch. Biochem. Biophys.* **2006**, *448*, 31–44. [[CrossRef](#)] [[PubMed](#)]
4. Hou, C.J.; Kulka, M.; Zhang, J.Z.; Li, Y.M.; Guo, F.J. Occurrence and biological activities of eremophilane-type sesquiterpenes. *Mini Rev. Med. Chem.* **2014**, *14*, 664–677. [[CrossRef](#)] [[PubMed](#)]
5. Becker, K.; Wongkanoun, S.; Wessel, A.C.; Bills, G.F.; Stadler, M.; Luangsa-ard, J.J. Phylogenetic and chemotaxonomic studies confirm the affinities of *Stromatoneurospora phoenix* to the *coprophilous xylariaceae*. *J. Fungi* **2020**, *6*, 144. [[CrossRef](#)]
6. Li, C.S.; Ding, Y.Q.; Yang, B.J.; Hoffman, N.; Yin, H.Q.; Mahmud, T.; Turkson, J.; Cao, S.G. Eremophilane sesquiterpenes from Hawaiian endophytic fungus *Chaetoconis* sp. FT087. *Phytochemistry* **2016**, *126*, 41–46. [[CrossRef](#)]
7. Khan, B.; Zhao, S.S.; Wang, Z.Y.; Ye, Y.H.; Rajput, N.A.; Yan, W. Eremophilane sesquiterpenes and benzene derivatives from the endophyte *microdiplodia* sp. WGHS5. *Chem. Biodivers.* **2021**, *18*, e2000949. [[CrossRef](#)]
8. Cheng, Z.B.; Zhao, J.J.; Liu, D.; Proksch, P.; Zhao, Z.M.; Lin, W.H. Eremophilane-type sesquiterpenoids from an *Acremonium* sp. fungus isolated from deep-sea sediments. *J. Nat. Prod.* **2016**, *79*, 1035–1047. [[CrossRef](#)]
9. Wu, Q.X.; Shi, Y.P.; Yang, L. Unusual sesquiterpene lactones from *Ligularia virgaurea* spp. *oligocephala*. *Org. Lett.* **2004**, *6*, 2313–2316. [[CrossRef](#)]
10. Liu, J.M.; Zhang, D.W.; Zhang, M.; Zhao, J.L.; Chen, R.D.; Wang, N.; Zhang, D.; Dais, J.G. Eremophilane Sesquiterpenes from an Endophytic Fungus *Periconia* Species. *J. Nat. Prod.* **2016**, *79*, 2229–2235. [[CrossRef](#)]
11. Kato, T.; Hirota, H.; Kuroda, C.; Gong, X.; Ohsaki, A. New eremophilane-type sesquiterpenes from *Ligularia cymbulifera*. *Nat. Prod. Commun.* **2017**, *12*, 1165–1167. [[CrossRef](#)]

12. Silchenko, A.S.; Kalinovsky, A.I.; Ponomarenko, L.P.; Avilov, S.A.; Andryjaschenko, P.V.; Dmitrenok, P.S.; Gorovoy, P.G.; Kim, N.Y.; Stonik, V.A. Structures of eremophilane-type sesquiterpene glucosides, alticolosides A-G, from the Far Eastern endemic *Ligularia Alticola Worosch.* *Phytochemistry* **2015**, *111*, 169–176. [[CrossRef](#)] [[PubMed](#)]
13. Bradfield, A.E.; Penfold, A.R.; Simonsen, J.L. The constitution of eremophilone and of two related hydroxy-ketones from the wood oil of *Eremophila mitchelli*. *J. Chem. Soc.* **1932**, 2744–2759. [[CrossRef](#)]
14. Yuyama, K.T.; Fortkamp, D.; Abraham, W.R. Eremophilane-type sesquiterpenes from fungi and their medicinal potential. *Biol. Chem.* **2018**, *399*, 13–28. [[CrossRef](#)]
15. Zhou, M.; Duan, F.F.; Gao, Y.; Peng, X.G.; Meng, X.G.; Ruan, H.L. Eremophilane sesquiterpenoids from the whole plant of *Parasenecio albus* with immunosuppressive activity. *Bioorg. Chem.* **2021**, *115*, 105247. [[CrossRef](#)]
16. Chen, J.; Chen, C.; Yao, X.; Jin, X.; Gao, K. Eremophilane-type sesquiterpenoids with diverse skeletons from *Ligularia sagittal.* *J. Nat. Prod.* **2014**, *77*, 1329–1335. [[CrossRef](#)]
17. Liu, M.Y.; Li, P.L.; Tang, X.L.; Luo, X.C.; Liu, K.C.; Zhang, Y.; Wang, Q.; Li, G.Q. Lemnardosinanes A-I: New bioactive sesquiterpenoids from soft coral *Lemnalia* sp. *J. Org. Chem.* **2021**, *86*, 970–979. [[CrossRef](#)]
18. Wu, G.W.; Lin, A.Q.; Gu, Q.Q.; Zhu, T.J.; Li, D.H. Four new chloro-eremophilane sesquiterpenes from an antarctic deep-sea derived fungus, *penicillium* sp. PR19N-1. *Mar. Drugs.* **2013**, *4*, 1399–1408. [[CrossRef](#)]
19. Lin, L.B.; Jian, X.; Qiang, Z.; Rui, H.; Xu, B.; Yang, S.X.; Han, W.B.; Tang, J.J.; Gao, J.M. Eremophilane sesquiterpenoids with antibacterial and anti-inflammatory activities from the endophytic fungus *Septoria rudbeckiae*. *J. Agric. Food Chem.* **2021**, *69*, 11878–11889.
20. Wang, A.; Yin, R.Y.; Zhou, Z.Y.; Gu, G.; Dai, J.G.; Lai, D.W.; Zhou, L.G. Eremophilane-type sesquiterpenoids from the endophytic fungus *Rhizopycnis vagum* and their antibacterial, cytotoxic, and phytotoxic activities. *Front. Chem.* **2020**, *8*, 596889. [[CrossRef](#)]
21. Amaral, L.S.; Rodrigues, E. Two novel eremophilane sesquiterpenes from an endophytic xylariaceous fungus isolated from leaves of *Cupressus lusitanica*. *J. Braz. Chem. Soc.* **2010**, *21*, 1446–1450. [[CrossRef](#)]
22. Xu, Y.J.; Nan, Z.D.; Li, W.H.; Huang, H.L.; Yuan, C.S. New eremophilanolides from *Ligularia hodgsonii*. *Helv. Chim. Acta* **2009**, *92*, 209–216. [[CrossRef](#)]
23. Liu, Q.; Shen, L.; Wang, T.T.; Chen, C.J.; Qi, W.Y.; Gao, K. Novel modified furanoeremophilane-type sesquiterpenes and benzofuran derivatives from *Ligularia veitchiana*. *Food Chem.* **2010**, *122*, 55–59. [[CrossRef](#)]
24. Ye, K.; Lv, X.; Zhang, X.; Wei, P.P.; Li, Z.H.; Ai, H.L.; Zhao, D.K.; Liu, J.K. Immunosuppressive Isopimarane Diterpenes from Cultures of the Endophytic Fungus *Ilyonectria robusta*. *Front. Pharmacol.* **2022**, *12*, 766441. [[PubMed](#)]
25. Yang, H.X.; Wu, X.; Chi, M.J.; Li, Z.H.; Feng, T.; Ai, H.L.; Liu, J.K. Structure and cytotoxicity of trichothecenes produced by the potato-associated fungus *Trichothecium crotocinigenum*. *Bioorg. Chem.* **2021**, *111*, 104874. [[CrossRef](#)] [[PubMed](#)]
26. Zhang, X.; Yang, H.X.; Ye, K.; Wei, P.P.; Lv, X.; Fan, Y.Z.; Yang, Y.L.; Ai, H.L.; Liu, J.K. Oblongolides from endophytic fungus *Phoma bellidis* Neerg. harbored in *Tricyrtis maculata* (D. Don) J.F. Macbr. *Phytochemistry* **2022**, *198*, 113126. [[CrossRef](#)]
27. Chen, Y.; Sun, L.T.; Yang, H.X.; Li, Z.H.; Liu, J.K.; Ai, H.L.; Wang, G.K.; Feng, T. Depsidones and diaryl ethers from potato endophytic fungus *Boeremia exigua*. *Fitoterapia* **2020**, *141*, 104483.
28. Wavefunction Inc. *Spartan 14*; Wavefunction Inc.: Irvine, CA, USA, 2014.
29. Frisch, M.J.; Trucks, G.W.; Schlegel, H.B.; Scuseria, G.E.; Robb, M.A.; Cheeseman, J.R.; Scalmani, G.; Barone, V.; Mennucci, B.; Petersson, G.A.; et al. *Gaussian 09, Revision D.01*; Gaussian, Inc.: Wallingford, CT, USA, 2010.
30. Bruhn, T.; Schaumlöffel, A.; Hemberger, Y.; Bringmann, G. SpecDis: Quantifying the comparison of calculated and experimental electronic circular dichroism spectra. *Chirality* **2013**, *25*, 243–249. [[CrossRef](#)]
31. Jain, R.J.; Bally, T.; Rablen, P.R. Calculating accurate proton chemical shifts of organic molecules with density functional methods and modest basis sets. *J. Org. Chem.* **2009**, *74*, 4017–4023. [[CrossRef](#)]
32. Grimblat, N.; Zanardi, M.M.; Sarotti, A.M. Beyond DP4: An improved probability for the stereochemical assignment of isomeric compounds using quantum chemical calculations of NMR shifts. *J. Org. Chem.* **2015**, *80*, 12526–12534. [[CrossRef](#)]
33. Yu, W.W.; Ma, J.T.; He, J.; Li, Z.H.; Liu, J.K.; Feng, T. Cadinane sesquiterpenoids from the fungus *Antrodia albocinnamomea* and their inhibitory activity against nitric oxide production. *Phytochemistry* **2022**, *196*, 113081. [[CrossRef](#)] [[PubMed](#)]
34. Bhattacharya, G.; Dhar, T.K.; Bhattacharyya, F.K.; Siddiqui, K.A. Mutagenic action of phaseolinone, a mycotoxin isolated from *Macrophomina phaseolina*. *Aust. J. Biol. Sci.* **1987**, *40*, 349–353. [[CrossRef](#)] [[PubMed](#)]
35. Dhar, T.K.; Siddiqui, K.A.I.; Ali, E. Structure of phaseolinone, a novel phytotoxin from *Macrophomina phaseolina*. *Tetrahedron Lett.* **1982**, *23*, 5459–5462.